Supporting Information

pH-Driven Self-Sorting in a Four Component Host-Guest System

Nuno Basílio,* Johan Mendoza, Sandra Gago and A. Jorge Parola

LAQV-REQUIMTE, Departamento de Química, Faculdade de Ciências e Tecnologia, Universidade NOVA de Lisboa, 2829-516 Caparica, Portugal

Experimental Section

Cucurbit[7]uril and *trans*-chalcones were available from previous studies.[1] All other reagents are commercially available and were used as received. The pH of the solutions was adjusted with HCl and NaOH and measured with a Crison basic 20+ pH meter. UV/vis absorption spectra were recorded using a Varian Cary 100 Bio or a Varian Cary 5000 spectrophotometer. Circular dichroism absorption spectra were recorded on a Chirascan qCD spectrometer at 298 K under constant nitrogen flush. A quartz cell (optical pathlength = 1 cm) was used for spectral acquisition. Two scans were averaged with baseline correction during all measurements. Fluorescence spectra were recorded in a Perkin Elmer LS-45 spectrofluorimeter. NMR experiments were run on a Bruker AMX 400 instrument, operating at 400 MHz (1H) and 101 MHz (13C). The solutions for NMR were prepared in D_2O and the pD adjusted with DCl or NaOD. Corrections due to isotope effects were applied using the equation pD = pH* + 0.4, where pH* is the reading taken from the pH meter.[2]

Mathematical Models

The sequential 2:1 host:guest complexation can be described by the two equilibrium reactions shown in Scheme S1.

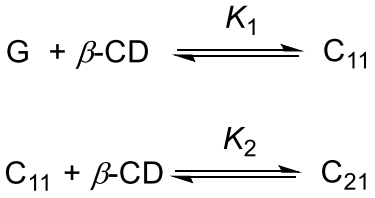

Scheme S1 – 2:1 sequential binding equilibria.

According to Scheme S1 the following equations can be written:

$$[G]_0 = [G] + [C_{11}] + [C_{21}] \qquad (S1)$$

$$[\beta\text{-}CD]_0 = [\beta\text{-}CD] + [C_{11}] + 2[C_{21}] \qquad (S2)$$

$$K_1 = \frac{[C_{11}]}{[\beta\text{-}CD][G]} \qquad (S3)$$

$$K_2 = \frac{[C_{21}]}{[\beta\text{-}CD][C_{11}]} \qquad (S4)$$

After some algebraic manipulations, the following equations are obtained:

$$[G] + K_1[\beta\text{-}CD][G] + K_1K_2[\beta\text{-}CD]^2[G] - [G]_0 = 0 \qquad (S5)$$

$$[\beta\text{-}CD] + K_1[\beta\text{-}CD][G] + 2K_1K_2[\beta\text{-}CD]^2[G] - [\beta\text{-}CD]_0 = 0 \qquad (S6)$$

The system of equations was solved numerically using the Newton-Raphson algorithm implemented in a conventional spreadsheet software to calculate the equilibrium concentrations of β-CD and G.[3] These values are used along with equations S3 and S4 to calculate the concentration of complexes for a given set of K_1 and K_2 values.

The observed chemical shifts (δ_{obs}) in the presence of host is given by mole fraction average of free and complexed guest given by equation S7 where δ_G is the chemical shift for the given proton signal in the absence of host, δ_{11} and δ_{21} are the limiting chemical shifts of the 11 and 21 complexes, respectively. The ^{1}H NMR data is fitted to equation S7, using the concentrations numerically determined and the Solver tool to optimize the K_1, K_2, δ_G, δ_{11} and δ_{21} parameters through a least squares minimization. The spreadsheet template is available from the authors upon request.

$$\delta_{obs} = \frac{\delta_G[G] + \delta_{11}[C_{11}] + \delta_{21}[C_{21}]}{[G]_0} \qquad (S7)$$

The same procedure can be used for fluorescence titrations using equation S8 where I_G, I_{11} and I_{21} are the limiting fluorescence intensities of the free guest, 1:1 complex and 2:1 complex, respectively.

$$I_{obs} = \frac{I_G[G] + I_{11}[C_{11}] + I_{21}[C_{21}]}{[G]_0} \qquad (S8)$$

The treatment of data for the pH dependent multicomponent mixture was also carried out using the Newton-Raphson algorithm implemented in a conventional spreadsheet software to calculate the equilibrium concentrations of all species from the binding constants and initial concentrations. The spreadsheet is also available from the authors upon request. The multistate equilibria are depicted in Scheme S2 for two general acids AH and BH that form complexes with two hosts β-CD and CB7 in their protonated and neutral (A and B) forms. It is worth noting that the acid-dissociation constant of the complexes (K'_a) is not required due to the relationship $K'_a = K_aK_A/K_{AH}$ that arises from

the cyclic nature of the thermodynamic schemes accounting for acid-base properties of host-guest systems.[4]

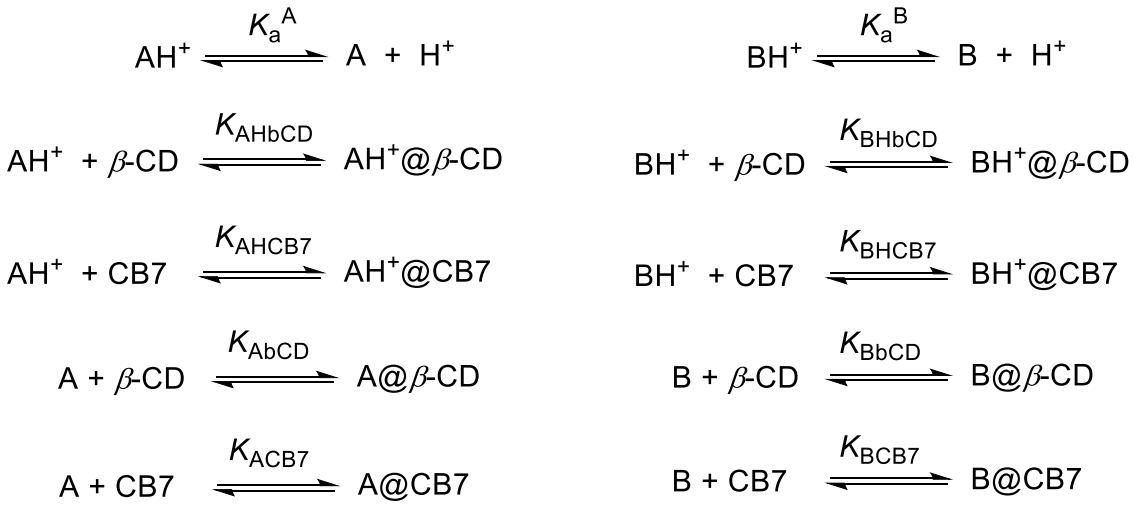

Scheme S2 – pH-dependent multistate equilibria in a four component host-guest system.

Considering Scheme S2 the mass balance expressions are given below:

$$[A]_0 = [A] + [AH^+] + [A@CB7] + [A@\beta\text{-}CD] + [AH^+@CB7] + [AH^+@\beta\text{-}CD] \qquad (S9)$$

$$[B]_0 = [B] + [BH^+] + [B@CB7] + [B@\beta\text{-}CD] + [BH^+@CB7] + [BH^+@\beta\text{-}CD] \qquad (S10)$$

$$[CB7]_0 = [CB7] + [A@CB7] + [B@CB7] + [AH^+@CB7] + [BH^+@CB7] \qquad (S11)$$

$$[\beta\text{-}CD]_0 = [\beta\text{-}CD] + [A@\beta\text{-}CD] + [B@\beta\text{-}CD] + [AH^+@\beta\text{-}CD] + [BH^+@\beta\text{-}CD] \qquad (S12)$$

And the equilibrium constants are defined by:

$$K_a^A = \frac{[A][H^+]}{[AH^+]}; \quad K_a^B = \frac{[B][H^+]}{[BH^+]};$$

$$K_{ACB7} = \frac{[A@CB7]}{[A][CB7]};\ K_{BCB7} = \frac{[B@CB7]}{[B][CB7]};\ K_{AHCB7} = \frac{[AH^+@CB7]}{[AH^+][CB7]};\ K_{BHCB7} = \frac{[BH^+@CB7]}{[BH^+][CB7]}$$

$$K_{AbCD} = \frac{[A@\beta\text{-}CD]}{[A][\beta\text{-}CD]};\ K_{BbCD} = \frac{[B@\beta\text{-}CD]}{[B][\beta\text{-}CD]};$$

$$K_{AHbCD} = \frac{[AH^+@\beta\text{-}CD]}{[AH^+][\beta\text{-}CD]};\ K_{BHbCD} = \frac{[BH^+@\beta\text{-}CD]}{[BH^+][\beta\text{-}CD]}$$

Rearranging equations S9-S12 a non-linear system of equations is obtained that can be solved numerically:

$$[A] + \frac{[A][H^+]}{K_a^A} + K_{ACB7}[A][CB7] + K_{AbCD}[A][\beta\text{-}CD] + K_{AHCB7}\frac{[A][H^+]}{K_a^A}[CB7] + K_{AHbCD}\frac{[A][H^+]}{K_a^A}[\beta\text{-}CD] - [A]_0 = 0 \qquad (S13)$$

$$[B] + \frac{[B][H^+]}{K_a^B} + K_{BCB7}[B][CB7] + K_{BbCD}[B][\beta\text{-}CD] + K_{BHCB7}\frac{[B][H^+]}{K_a^B}[CB7] + K_{BHbCD}\frac{[B][H^+]}{K_a^B}[\beta\text{-}CD] - [B]_0 = 0 \qquad (S14)$$

$$[CB7] + K_{ACB7}[A][CB7] + K_{BCB7}[B][CB7] + K_{AHCB7}\frac{[A][H^+]}{K_a^A}[CB7] + K_{BHCB7}\frac{[B][H^+]}{K_a^B}[CB7] - [CB7]_0 = 0 \qquad (S15)$$

$$[\beta\text{-}CD] + K_{AbCD}[A][\beta\text{-}CD] + K_{BbCD}[B][\beta\text{-}CD] + K_{AHbCD}\frac{[A][H^+]}{K_a^A}[\beta\text{-}CD] + K_{BHbCD}\frac{[B][H^+]}{K_a^B}[\beta\text{-}CD] - [\beta\text{-}CD]_0 = 0 \qquad (S16)$$

The solutions of the system of equation provides the equilibrium concentration of all free species that can be inserted in the equilibrium equations to determine the concentration of the complexes.

Spectroscopic Data

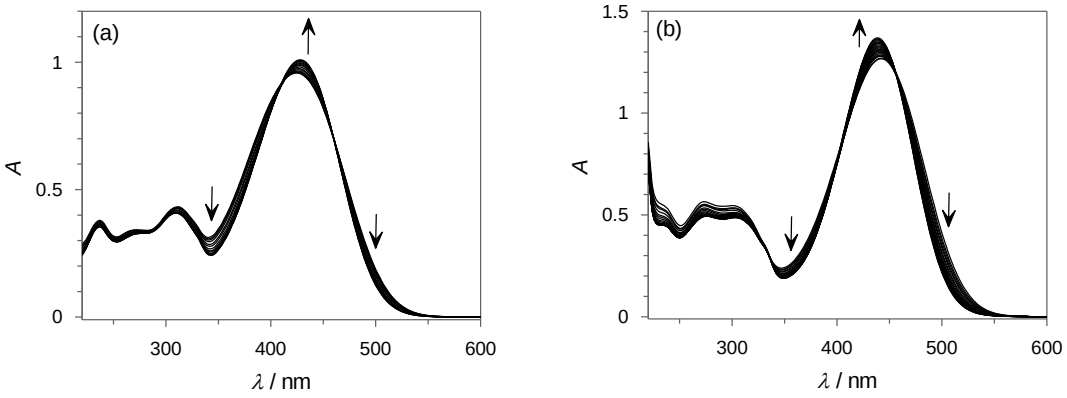

Figure S1- Absorption spectra of **1a** (a) and **1b** (b) in the presence of increasing concentrations of β-CD. The titration experiments where conducted at pH = 7 with [**1a**] = 40 μM, [**1b**] = 44 μM and 0 < [β-CD] < 0.01 M in both titrations.

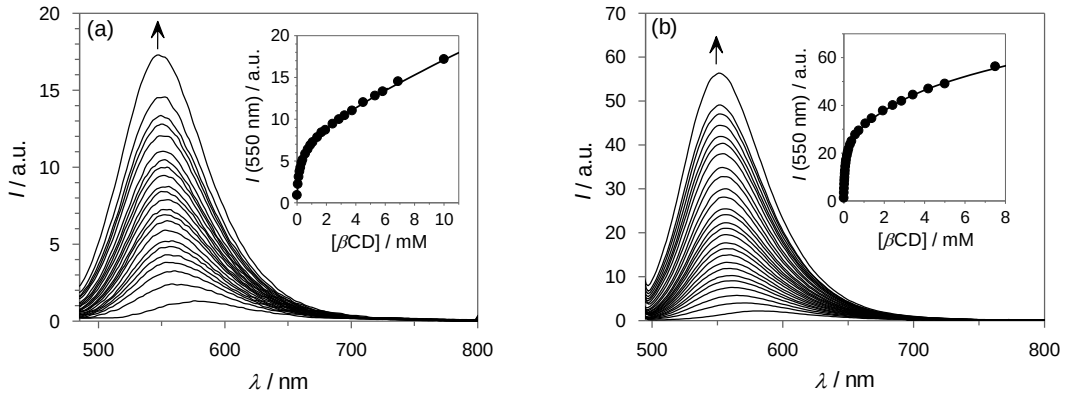

Figure S2- Emission spectra of **1a** (a) and **1b** (b) in the presence of increasing concentrations of β-CD. The titration experiments where conducted at pH = 7 with [**1a**] = 6.6 μM and [**1b**] = 8.9 μM. Excitation was carried out at an isosbestic point (462 and 457 nm for **1a** and **1b**, respectively).

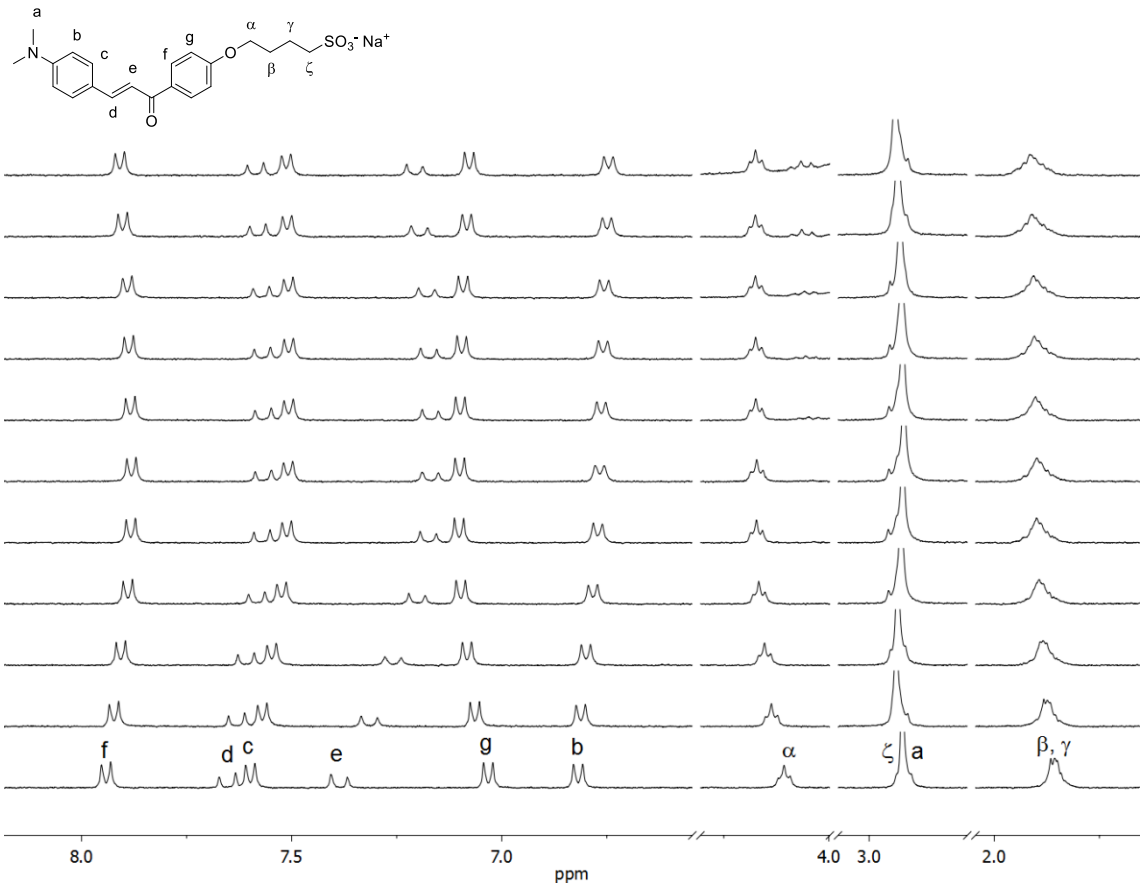

Figure S3- ^{1}H NMR spectra of **1a** (0.5 mM, pD = 7) in presence of increasing concentrations of *β*-CD from 0 (bottom) to 9 mM (top).

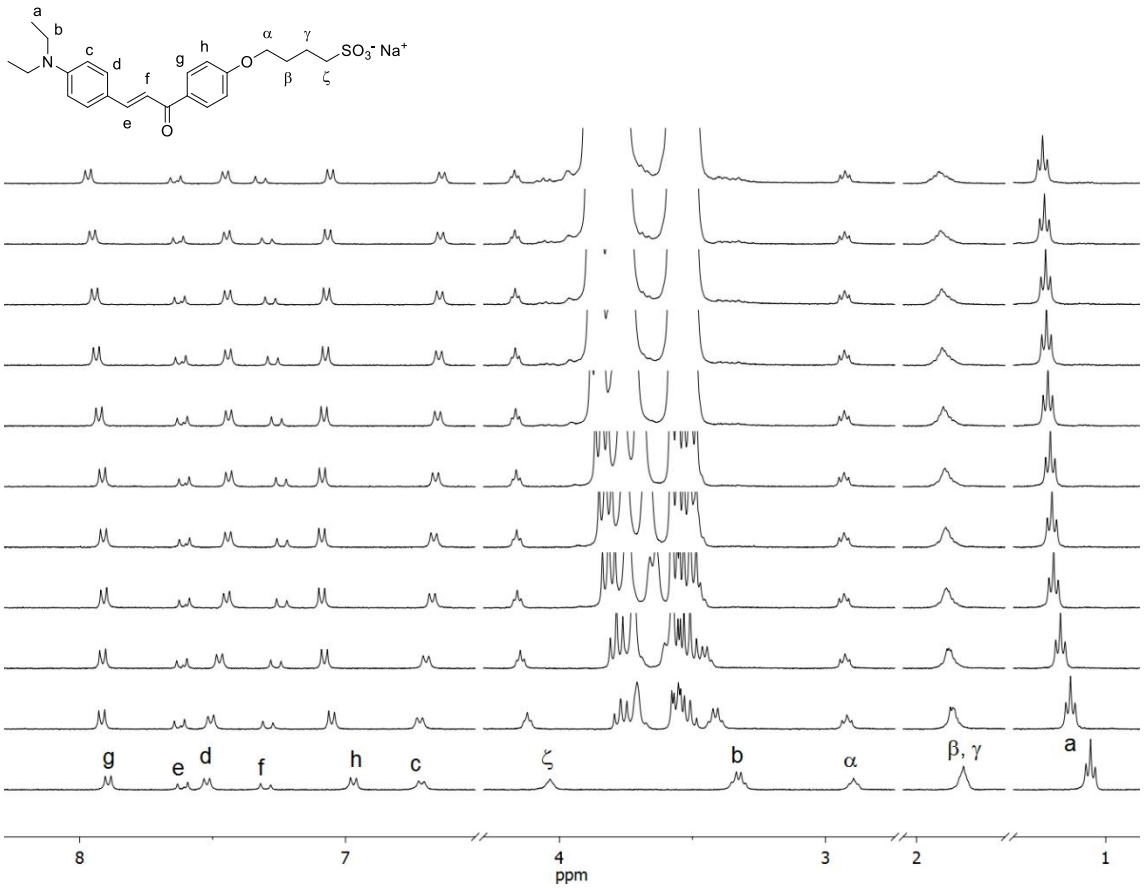

Figure S4- ^{1}H NMR spectra of **1b** (0.5 mM, pD = 7) in presence of increasing concentrations of β-CD from 0 (bottom) to 9 mM (top).

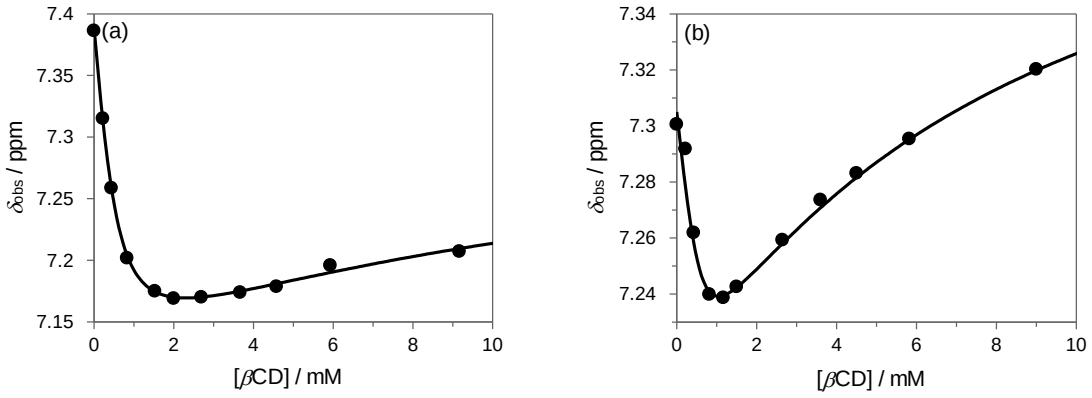

Figure S5- Observed ^{1}H NMR chemical shifts (δ_{obs}) of proton *e* and *f* of **1a** (a) and **1b** (b), respectively, plotted against the concentration of β-CD. The concentration of guest was 0.5 mM in both experiments.

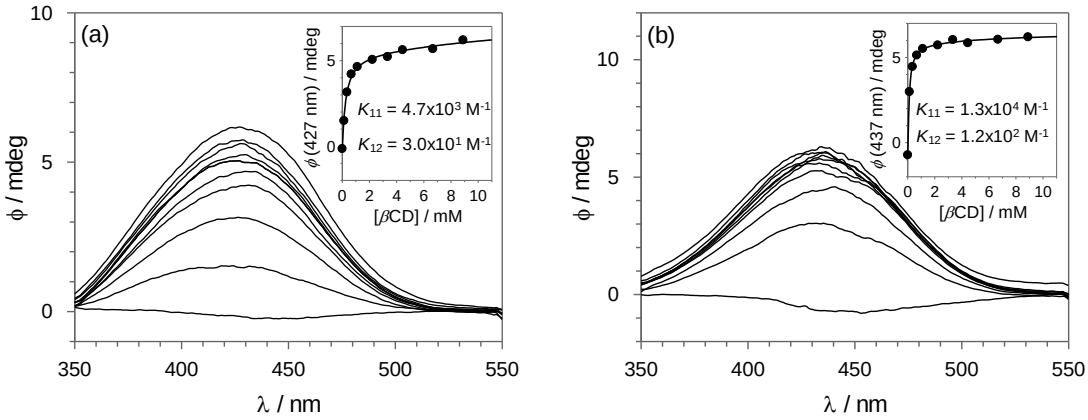

Figure S6- Circular dichroism spectra of **1a** (a) and **1b** (b) in the presence of increasing concentrations of β-CD. The titration experiments where conducted at pH = 7 with [**1a**] = 77 μM and [**1b**] = 68 μM.

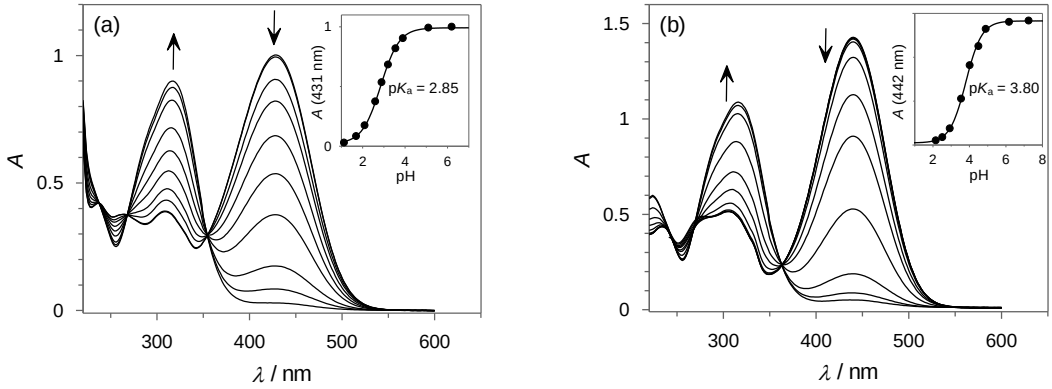

Figure S7- (a) Spectral modifications observed upon gradual pH variations in an aqueous solution of **1a** (40 μM) in presence of 2 mM of β-CD and (b) the same for **1b** (44 μM) with 2 mM of β-CD.

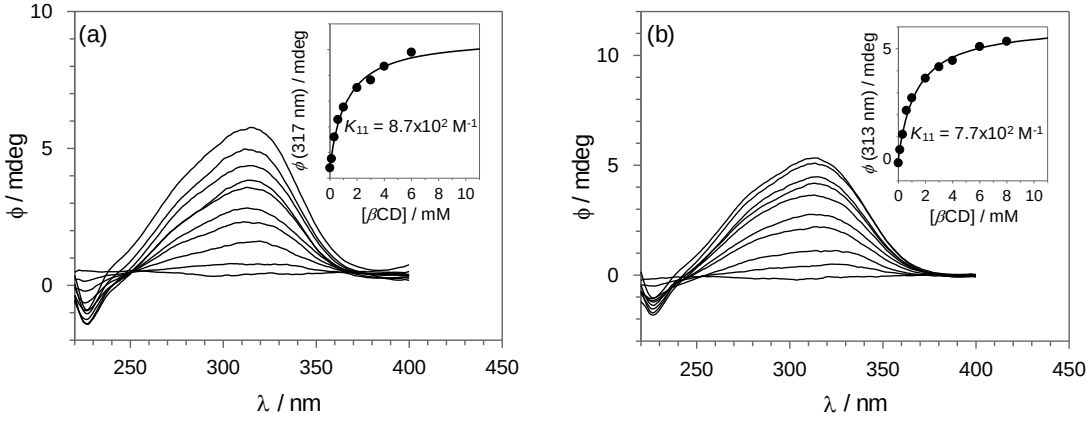

Figure S8- Circular dichroism spectra of **1a** (a) and **1b** (b) in the presence of increasing concentrations of β-CD. The titration experiments where conducted at pH = 1 with [**1a**] = 77 μM and [**1b**] = 68 μM.

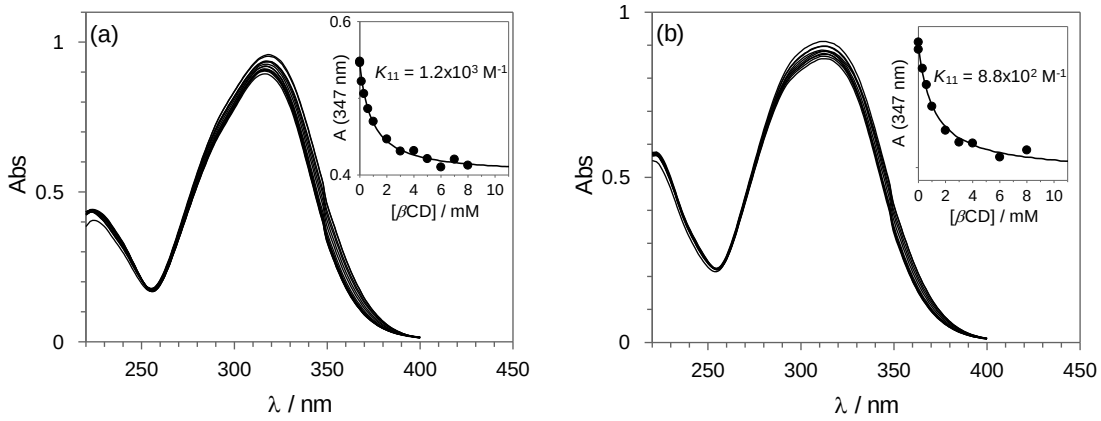

Figure S9- UV-vis absorption spectra of **1a** (a) and **1b** (b) in the presence of increasing concentrations of β-CD. The titration experiments where conducted at pH = 1 with [**1a**] = 40 μM and [**1b**] = 40 μM.

Comments to the Job plot method: this method has serious limitations that were recognized in recent works.[5,6] It is now accepted that this technique is not conclusive and in some cases may lead to misinterpretations. The chalcone-cyclodextrin complexation reported in this paper is one of these cases due to the small fraction of 2:1 complexes (see figure S10b and S11b). As can be observed in figure S10a the data showing a maximum at 0.5 can be simulated with a 2:1 complexation model. Thus, while deviation from 0.5 may suggest higher stoichiometries the observation of a maximum at 0.5 does not confirm exclusive 1:1 binding mechanism.

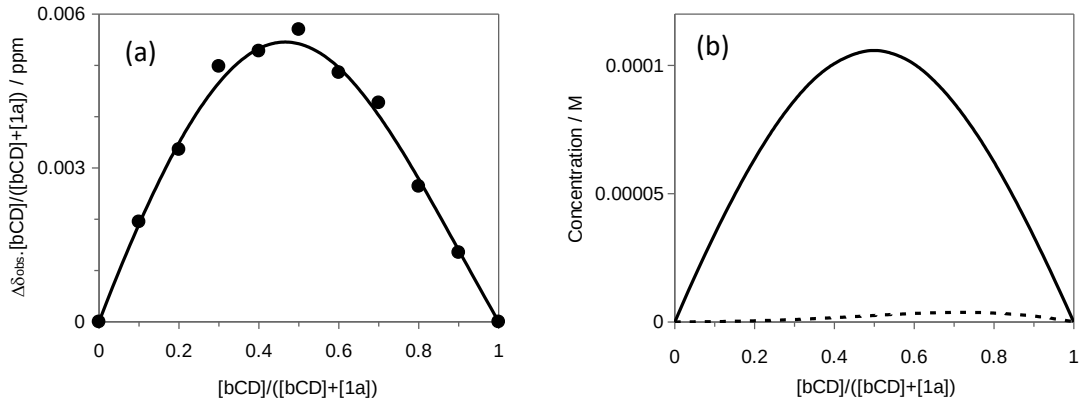

Figure S10- (a) Job plot for the complexation of **1a** and β-CD constructed from the proton NMR signal H1 of β-CD. The total concentration was kept constant and [β-CD]+[**1a**] = 0.5 mM. (b) Variation on the concentration of complexed β-CD species under the Job's Plot conditions. Full line - 1:1 complexes and dotted line – 2:1 complexes (this was multiplied by 2 to account for the β-CD stoichiometry).

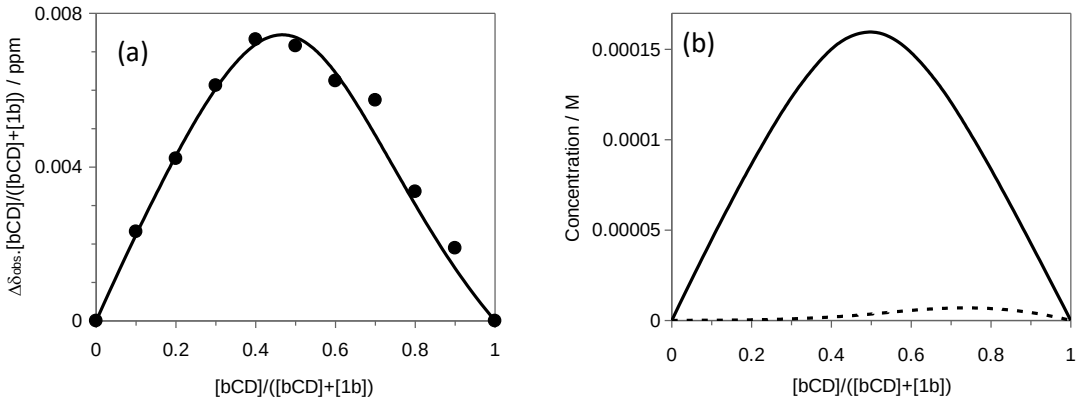

Figure S11- (a) Job plot for the complexation of **1b** and *β*-CD constructed from the proton NMR signal H1 of *β*-CD. The total concentration was kept constant and [*β*-CD]+[**1b**] = 0.5 mM. (b) Variation on the concentration of complexed *β*-CD species under the Job's Plot conditions. Full line - 1:1 complexes and dotted line – 2:1 complexes (this was multiplied by 2 to account for the *β*-CD stoichiometry).

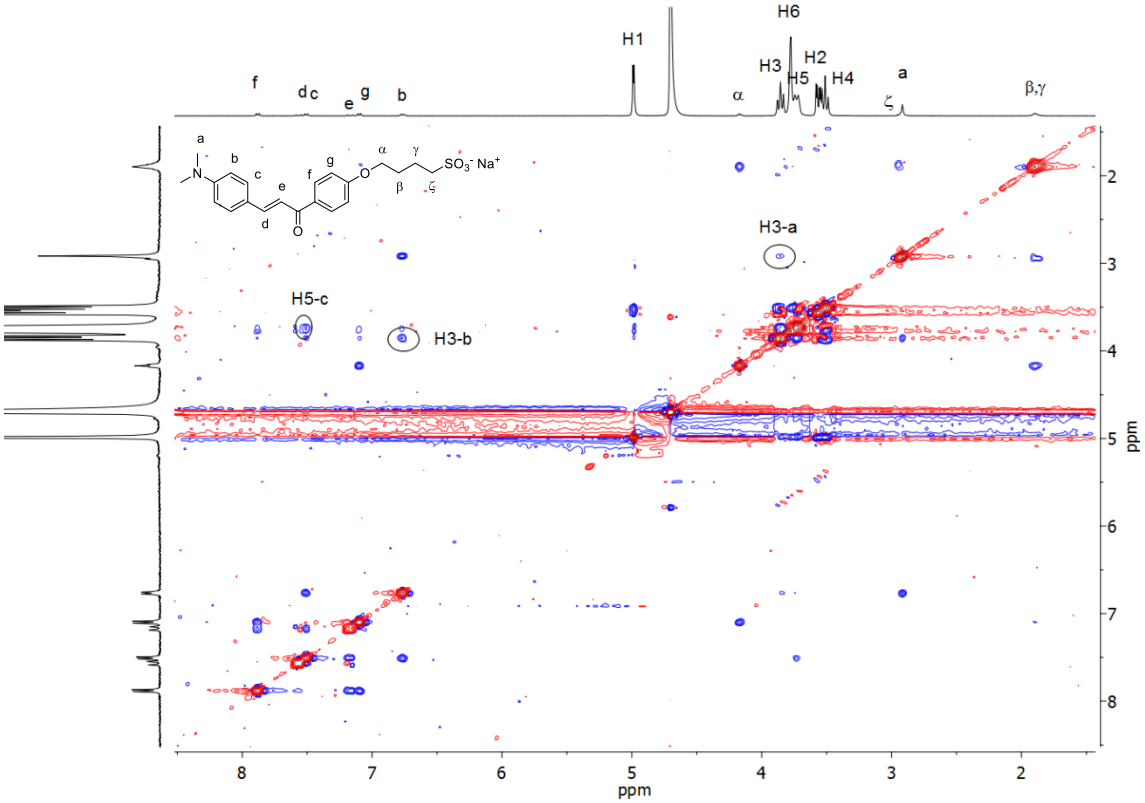

Figure S12- ROESY spectrum of **1a** (0.5 mM, D_2O) in presence of 2 mM of *β*-CD.

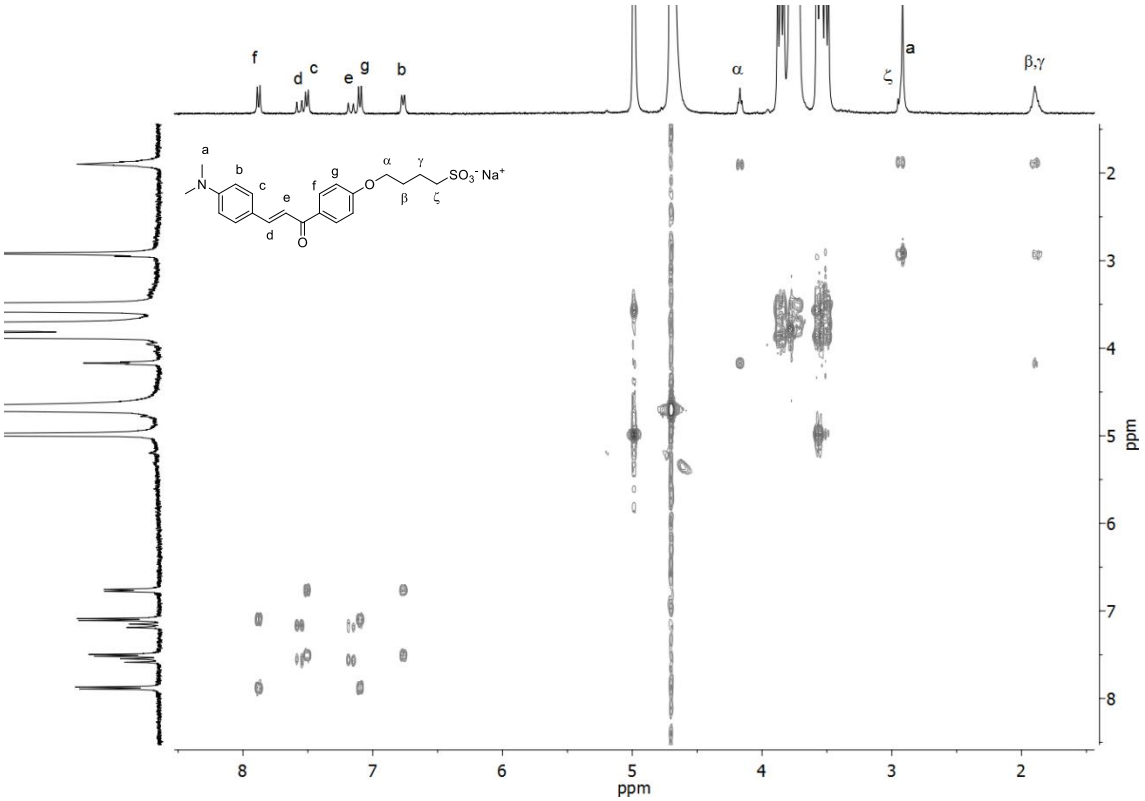

Figure S13- COSY spectrum of **1a** (0.5 mM, D_2O) in presence of 2 mM of *β*-CD.

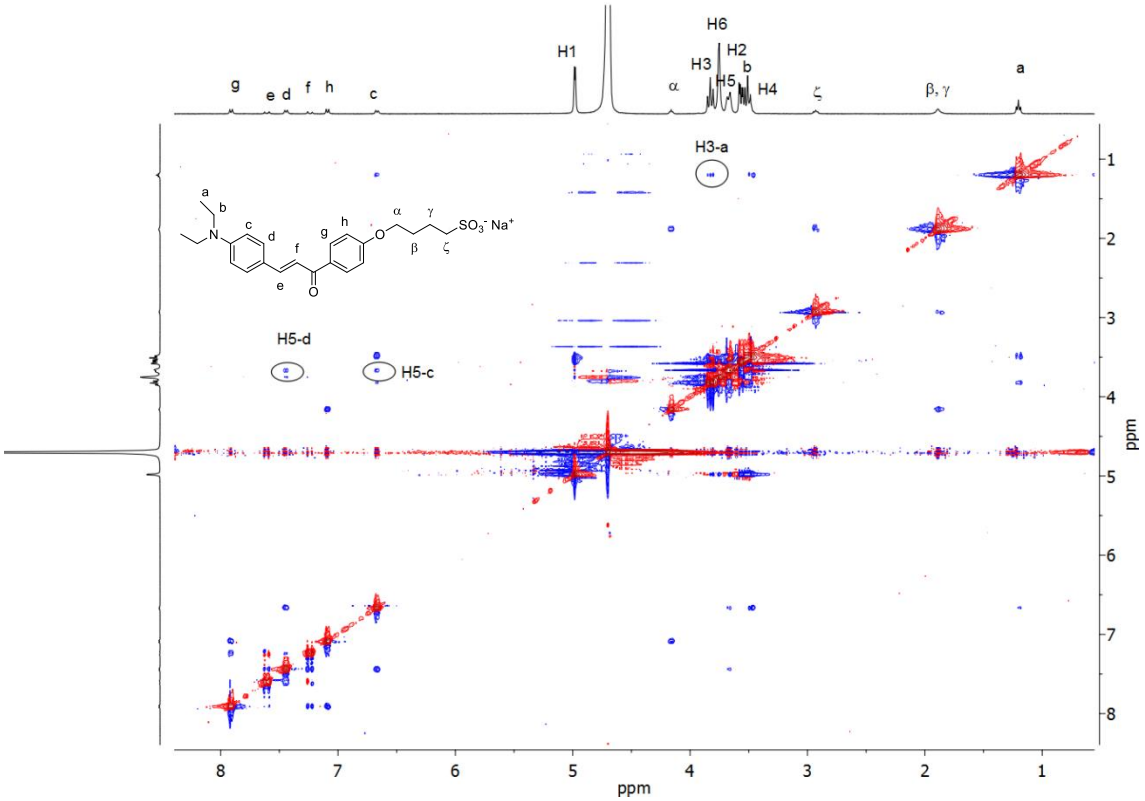

Figure S14- ROESY spectrum of **1b** (0.5 mM, D_2O) in presence of 2 mM of *β*-CD.

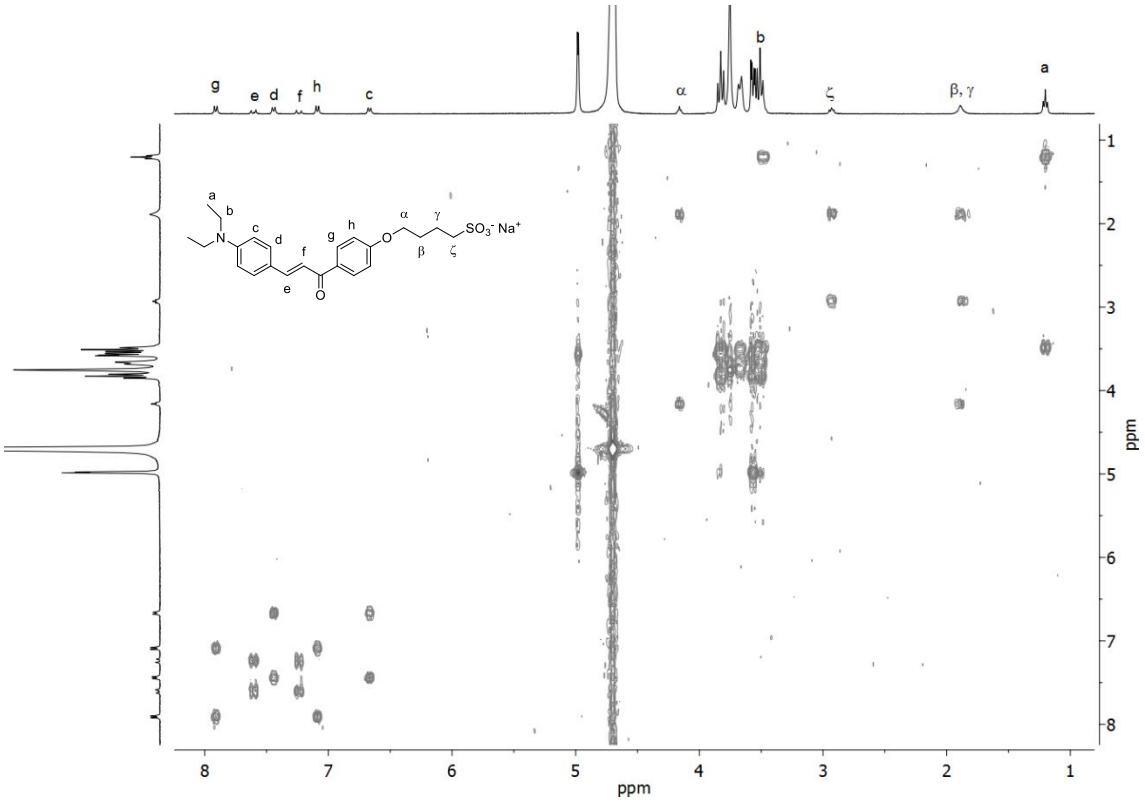

Figure S15- COSY spectrum of **1b** (0.5 mM, D_2O) in presence of 2 mM of β-CD.

Control Experiments

The four component mixture was further analyzed at 5 ºC with equimolar concentrations (0.5 mM) and pD = 2 by ^{1}H NMR (Figure S16). Decreasing the temperature improve the signal resolution showing the diagnosing signals of the complex **1a** with CB7 and at the same time the peaks (still broaden due to residual binding with CB7) of **1b** with *β*-CD. For and equimolar mixture, the selective binding of **1a** by CB7 leaves **1b** free. The last will necessarily bind to *β*-CD (as **1a** is not available) in agreement with the predicted self-sorting behavior.

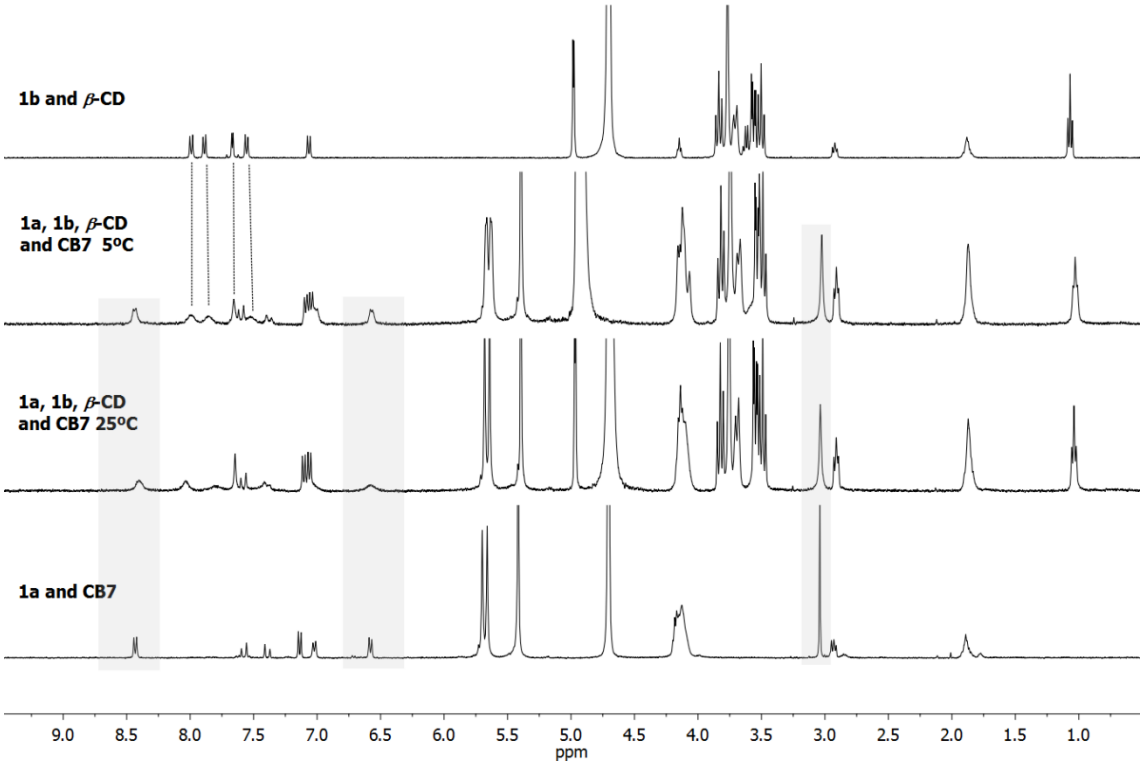

Figure S16- ^{1}H NMR spectra of (bottom to the top):1- **1a** and CB7 at 25 ºC; 2- four component mixture containing **1a**, **1b**, *β*-CD and CB7 at 25 ºC; 3- four component mixture containing **1a**, **1b**, *β*-CD and CB7 at 5 ºC; 4- **1b** and *β*-CD at 25 ºC. The concentration of the different species was fixed at 0.5 mM in all experiments and conducted in D_2O with pD = 2.

To demonstrate that ^{1}H NMR signal broadening occurs due to residual binding, an equimolar solution of **1b** and *β*-CD was titrated with CB7 and monitored by ^{1}H NMR

(Figure S17). As can be observed, for 0.11 equivalents of CB7 (second spectrum from the bottom) the signals broaden significantly. In this case the relative concentrations of **1b**-CB7 complex cannot be higher than 11%. This experiment supports that the residual complexation of **1b**-CB7 in the four-component mixture can be around 10% as predicted in our simulation (Figure 1b and 1e in the manuscript). The complexation-induced chemical shifts of proton *a* of **1b** and H1 of *β*-CD (Figure S18) were fitted with the theoretical model (see above) using the *K* values reported in Table 1 of the manuscript for this guest at acidic pH. As can be observed the experimental data shows perfect agreement with the theoretical model (in the absence of **1a** the model is equivalent to a competitive mechanism with two hosts). In addition, the observed changes in the ^{1}H NMR signal of *β*-CD suggest the formation of a complex that dissociates upon addition of CB7 due to competitive binding.

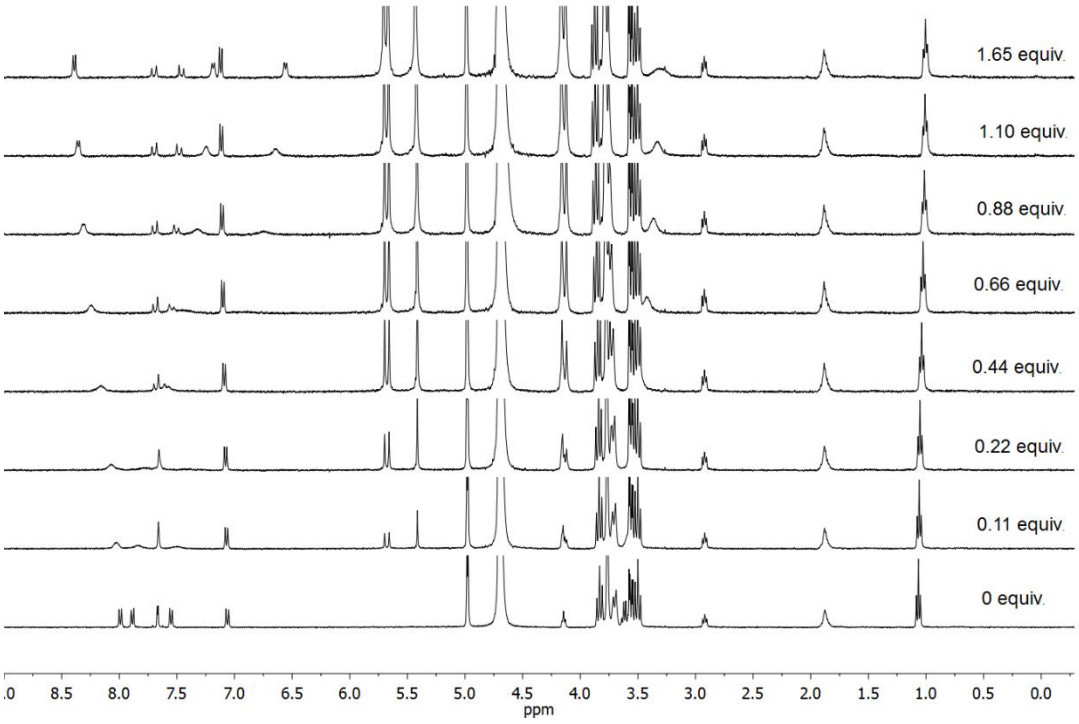

Figure S17- ^{1}H NMR spectra of equimolar mixture of **1b** and *β*-CD with increasing concentrations of CB7. The initial concentrations of **1b** and *β*-CD were 0.5 mM and were slightly diluted during CB7 additions. All experiments were conducted in D_2O with pD = 2.

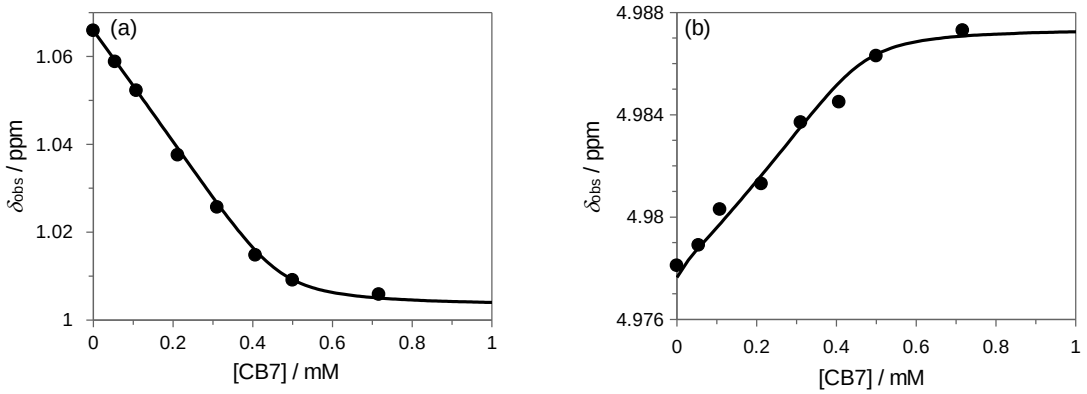

Figure S18- (a) Observed ^{1}H NMR chemical shifts (δ_{obs}) of proton *a* of **1b** and (b) proton H1 of β-CD plotted against the concentration of CB7. The initial concentration of **1b** and β-CD were 0.5 mM. The experimental conditions are described in the caption of Figure S17.

Figure S19 shows the variation in the ^{1}H NMR spectra of an equimolar mixture of **1a**, **1b** and β-CD as function of the CB7 concentration. The results provide strong evidence for the self-sorting system described in the manuscript. As can be observed the signals of **1a** (red lines) start to shift at concentrations of CB7 below 1 equivalent while the signals of **1b**, despite of broadening, are kept practically constant at the same frequency. This suggests strong selectivity of CB7 for **1a** over **1b**. On the other hand, above 1 equivalent the resonances of **1a** did not show further complexation induced shifts while those of **1b** start to shift significantly. This behavior is strongly suggestive of the sequential binding predicted by our model and represented in Figure 1b of the manuscript. As in Figure S18, Figure S20 shows the complexation induced chemical shifts of proton *a* of **1b** and H1 of β-CD fitted with the theoretical model accounting for the complexation phenomena in the four-component host-guest system. As can be observed the experimental data is satisfactorily described by the model using the *K* values reported in Table 1 of the manuscript at acidic pH values. During the fitting procedure the *K* values were fixed and the limiting chemical shifts of **1b** species (equation S17; Figure S20a) and β-CD species

(equation S18; Figure S20b) were optimized. Figure S20a shows the above described behavior: no binding of **1b** below 0.5 mM of CB7 due to selective binding of **1a** and binding of the first after quantitative complexation of the second. On the other hand, the chemical shifts variations observed for the *β*-CD signals (Figure S20b) are indicative of the complexation of **1a** and **1b** with this host in the absence of CB7 and dissociation of this weaker complexes with the addition of the high affinity host. Obviously, the sequential selective complexation of **1a** and of **1b** (Figure S20a) implies sequential dissociation of the *β*-CD complexes and supports the self-sorting phenomena under equimolar conditions.

$$\delta_{obs} = \frac{\delta_{1b}[1b] + \delta_{1b\text{-}\beta CD}[1b\text{-}\beta CD] + \delta_{1b\text{-}CB7}[1b\text{-}CB7]}{[1b]_0} \qquad (S17)$$

$$\delta_{obs} = \frac{\delta_{\beta CD}[\beta CD] + \delta_{1a\text{-}\beta CD}[1a\text{-}\beta CD] + \delta_{1b\text{-}\beta CD}[1b\text{-}\beta CD]}{[\beta CD]_0} \qquad (S18)$$

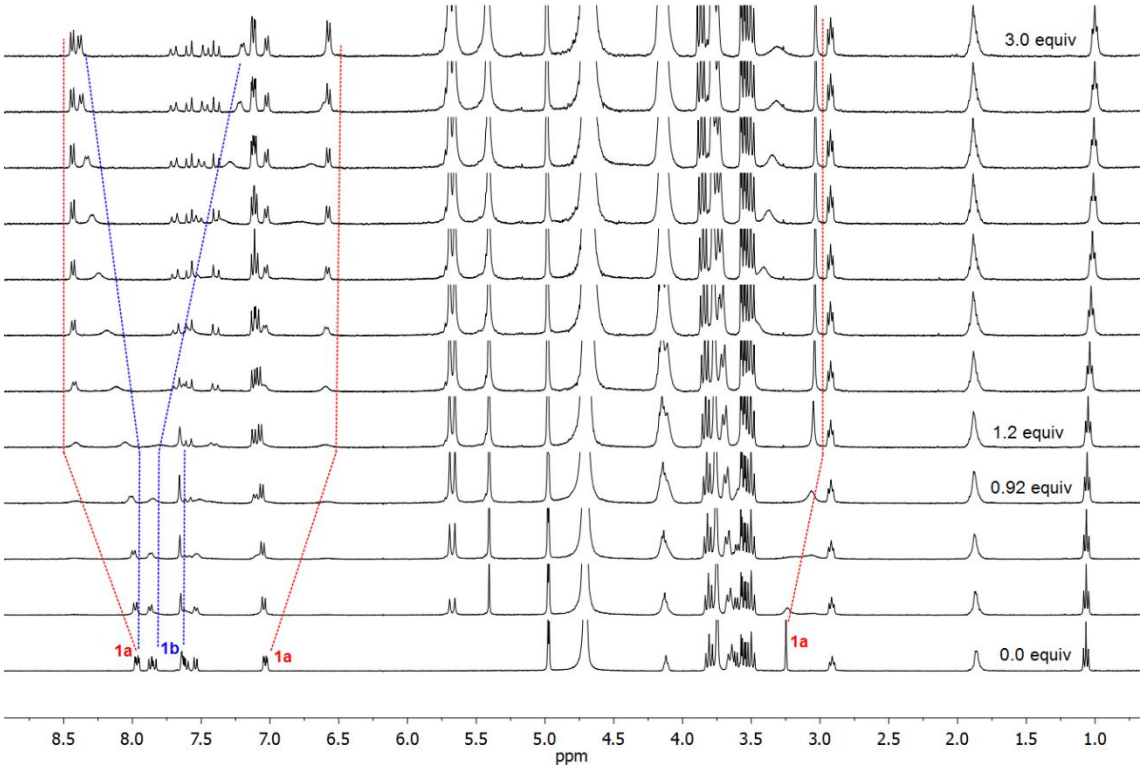

Figure S19- ^{1}H NMR spectra of a mixture of **1a**, **1b** and *β*-CD with increasing concentrations of CB7. The concentration of **1a**, **1b** and *β*-CD was 0.5 mM and kept constant during the CB7 titrations. All experiments conducted in D_2O with pD = 2.

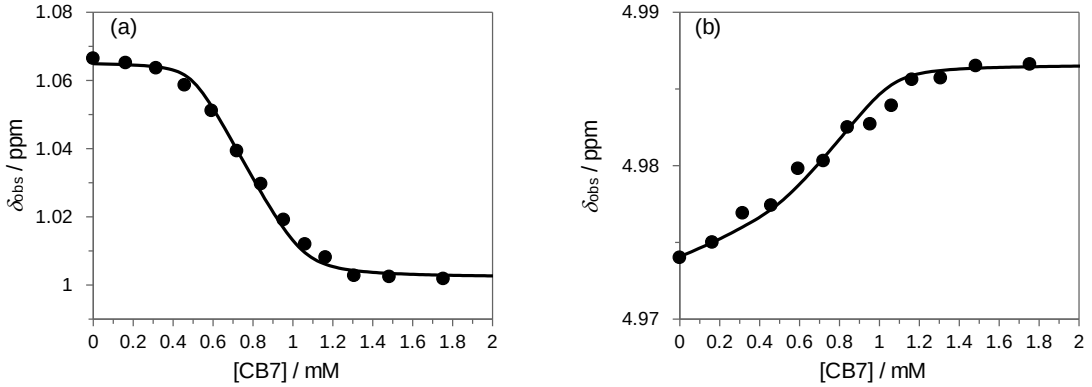

Figure S20- (a) Observed ^{1}H NMR chemical shifts (δ_{obs}) of proton *a* of **1b** and (b) proton H1 of β-CD plotted against the concentration of CB7. The data was taken from the spectra of Figure S19.

REFERENCES

1 N. Basílio, S. Gago, A. J. Parola and F. Pina, *ACS Omega*, 2017, **2**, 70–75.

2 P. K. Glasoe and F. A. Long, *J. Phys. Chem.*, 1960, **64**, 188–190.

3 S. del Piero, A. Melchior, P. Polese, R. Portanova and M. Tolazzi, *Ann. Chim.*, 2006, **96**, 29–49.

4 J. Mohanty, A. C. Bhasikuttan, W. M. Nau and H. Pal, *J. Phys. Chem. B*, 2006, **110**, 5132–5138.

5 D. Brynn Hibbert and P. Thordarson, *Chem. Commun.*, 2016, **52**, 12792–12805.

6 F. Ulatowski, K. Dąbrowa, T. Bałakier and J. Jurczak, *J. Org. Chem.*, 2016, **81**, 1746–1756.